Analysis of the Skeleton Sled Sliding Motion Induced Vibrations with Different Runner Stiffness's on an Inclined Ice Track

Martins Irbe, Karlis Agris Gross, Janis Viba, and Marina Cerpinska

Abstract The skeleton is one of the winter Olympics games sports and it is the only sport where is possible to alter the degree of contact with ice by altering the runner stiffness. Stiffness increased by compressing the ends of the runners resulting in less contact with the ice. Beginners prefer a runner setting with a lower stiffness for greater stability. Experienced winter athletes will select a higher stiffness for higher speeds, but this comes at the cost of less control of slider motion on the ice. Sliding motion induced vibrations are not very obvious but can play a quite positive role in reducing the sliding friction. The purpose of this research is to identify skeleton sled vibrations that are characterized by natural frequencies of the structure and which are characterizing sliding motion friction forces and compare them with different runner stiffness. Analyzing the effect of structural vibrations from the sliding motion on the ice surface first is clarified how the sliding object responds on forced oscillations. Using CAD Simulation software the first natural frequencies were detected for skeleton sled and runners. Values were compared with laboratory measuring equipment data. Practical experiments were performed in ice track at the bobsled push-start facility in Sigulda, Latvia and it was conducted on a straight 23.7 m long ice track angled at $\alpha = 12°$. The sliding time was measured with optical sensors at the top and bottom of the incline after the skeleton starts from sliding from a stationary position. This sliding time was used to calibrate the accelerometer data. Measurements were made with portable accelerometer, it was fixed to the base plate of skeleton. Data was processed by spectral analysis. Then motion and structure characterizing frequencies

M. Irbe (✉) · K. A. Gross
Biomaterials Research Laboratory, Riga Technical University, Riga, Latvia
e-mail: Martins.Irbe@rtu.lv

K. A. Gross
e-mail: Karlis-Agris.Gross@rtu.lv

M. Irbe · J. Viba · M. Cerpinska
Institute of Mechanics and Machine Building, Riga Technical University, Riga, Latvia
e-mail: Janis.Viba@rtu.lv

M. Cerpinska
e-mail: Marina.Cerpinska@rtu.lv

E. J. Sapountzakis et al. (eds.), *Proceedings of the 14th International Conference on Vibration Problems*, Lecture Notes in Mechanical Engineering,
https://doi.org/10.1007/978-981-15-8049-9_6

were obtained. The results were analyzed by comparing computer calculations and simulations with practical experiments. The acceleration data analysis confirmed that the natural frequency of skeleton sleigh structure does not change as the sleigh's runner stiffness changes. 3D modeling certified that the change was minimal if the connection type was not altered. The created mathematical model for determining natural frequencies allows to quickly and accurately determine the first modes of the oscillations of the structure.

Keywords Winter sports · Skeleton · Structural vibrations · Induced vibrations · Sliding motion

1 Introduction

The structure of the skeleton sleigh is designed so that both it's runners act as tensioned springs between the rider and the ice surface. This is a fundamental difference to other winter sliding sports' equipments. This means that the runners are exposed to complex loads during the race, i.e., there are considerably greater local deformations; the runners are pressed and bent at the entrances and exits of the track curves; they are exposed to various vibrations while overcoming the undulations of the ice.

One of the peculiarities of the skeleton runner's construction is that it is possible to adjust the tension of the runners within a certain range before the race, by tightening the ends of the runners with a compression screw, resulting in a change of radius of the curvature.

For example, young athletes initially select the radius of runner's curvature to be r = 6 mm, while experienced athletes who participate in significant races choose the curvature between 11, 12, and even 13 mm. This means that the bigger the radius of the curvature, the better the slideability—because the contact surface area reduces. But the payback for reduced contact area is a decreased ability to control the skeleton sleigh on the track curves. Athletes often risk and improve the slideability, but therefore lose some ability to control the sleigh and may even fall. Meanwhile winter sliding sports have certain constructive rules, which are regulated by the international federations and institutions of the respective sports. In skeleton it is FIBT [1].

This study was conducted at the Winter Sports Center in Sigulda Bobsled push-start facility, in co-operation with the Latvian Olympic Skeleton team. The main task of the study was to determine how the change of stiffness of the skeleton runner affects the natural of the skeleton sleigh structure. Experimental measurements of acceleration were performed for skeleton sleighs on an inclined 24 m long ice track. After the processing of the experimental data the main dominant frequencies were obtained. In the analysis of the data, frequencies related to the frictional motion processes and additional frequencies related to the structure's induced oscillations were identified. All experiments were performed at different runner's stiffness values,

which were regulated on the experiments with radius of the curvature r. In parallel, the results were compared and analyzed with computer simulation in 3D. In addition, a simplified mathematical model of natural frequency determination in 1D space for 6DOF chain type system has been developed.

Previous studies have been launched at the Winter Sports Center in Sigulda, modeling the dynamics of skeleton sleigh's sliding motion [2]. In this work two-dimensional mathematical model describing the movement skeleton sleighs was created. The model has been verified experimentally on the ice track with acceleration measurement data. In this model, the influence of many parameters on sliding velocity has been studied in depth, such as c—stiffness of the skeleton sleigh's runner; μ—coefficient of friction of ice; C_D—the force of aerodynamic resistance. The started research work continued with in-depth analysis of runner's stiffness changes. For this purpose, the runner was divided into several elements connected with rotational spring pins. The parameters of the spring stiffness were changed and their impact on sliding was analyzed. The results showed a high degree of nonlinearity.

Studies related to sliding improvement in winter sports have been explicitly discussed and summarized by Braghin et al. [3]. In all winter sliding sports, the main task is to reduce the time spent on the track. Research began with a review of present literature on the impact of vibration on slideability. In works [4, 5] it has been experimentally proven that at high loading frequencies the friction coefficient between ice or snow and the surface of the test sample significantly reduces. It was also proven mathematically. There are vibrations excited by the dynamic component of an externally applied normal load. The average normal contact deflection during oscillations is smaller than the static deflection under the same average load that calls Hertzian stiffness [6, 7]. It is shown that the maximum average friction reduction without contact loss is approximately ten percent.

A large-scale study on skeleton sports has been carried out in the Ph.D. thesis [8]. It was analyzed how the athlete runs the start-up run and lands on the sleigh surface and how the motion was influenced by the sliding trajectories. The accelerometer was used for measurements of overall values, but no vibration data was analyzed. As the skeleton's sleigh differs significantly from the rest of winter sliding sports' sleighs, they were not discussed in detail in this Ph.D. thesis.

In this study theoretical materials [9–13] were used for the vibration analysis to accomplish working with the 3D modeling software SolidWorks Simulation and mathematical calculations. Using SolidWorks Simulation the first natural frequencies were detected for skeleton sled. Every structure has its natural frequencies of vibration called resonant frequencies. Each such frequency is characterized by a specific shape of vibration time wave. When excited with a resonant frequency, a structure vibrates and acquires specific shape, which is called vibration mode. In statics natural frequency is calculated knowing the relation between the mass properties of the structure and its stiffness. During the resonance, inertial an elastic stiffness is neglected. The sole factor controlling the vibration amplitude is damping. If damping is low, the amplitude may rise dramatically. In real life, a structure has an infinite number of natural frequencies and only a few of the lowest modes are important for analysis of the response of the structure to the dynamic loading.

2 Experiment of the Skeleton on the Ice Track and Runner Compression Test

The experiment was conducted on a straight 23.7 m long ice track angled at $\alpha = 12°$. Figure 1 on the left shows the location of the accelerometer fixed to the underside of the skeleton at the center of mass. For the frequency analysis, data was collected by 3-axial portable Accelerometer X16-1D. The data recording speed was 400 Hz. The skeleton together with added mass was slid down the ice track at the Bobsled push-start facility in Sigulda, Latvia.

The mass of the sled is 35 kg, the added mass is 65 kg, and the weight of the measuring device is 48 g. The sliding time was measured with optical sensors at the top and bottom of the incline after the skeleton started sliding from a stationary position. This sliding time was used to calibrate the accelerometer data.

Figure 2 shows the reference position when radius of the curvature is zero, $r = 0$ mm, the runner is completely non-tensioned, $F = 0$ N; and runner compression displacement is zero, $\Delta = 0$ mm. There were 11 stiffness positions selected based on the athlete's experience. Defined range was from 7 to 12 mm with a step of 0.5 mm. In each stiffness position, 3 runs were performed, 33 runs in total. Experiments were designed to be done in the shortest possible time interval, in the middle of the day, in similar weather conditions.

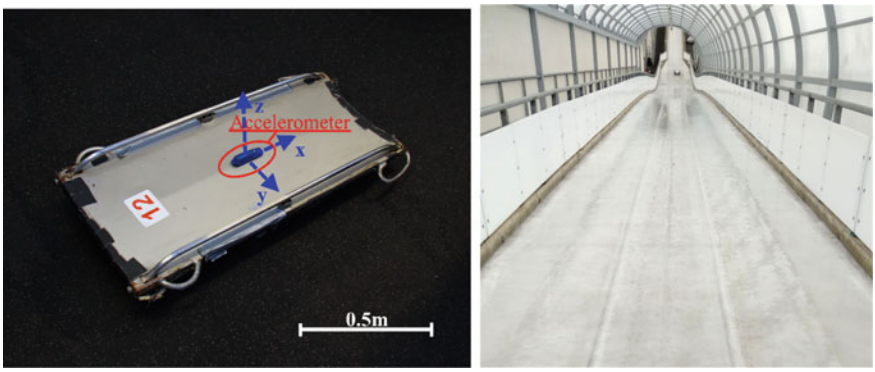

Fig. 1 Skeleton with portable accelerometer and the Bobsled push-start facility in Sigulda, Latvia

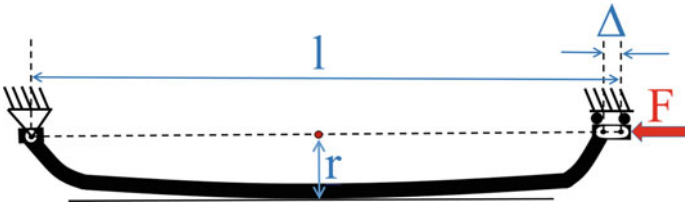

Fig. 2 The runner tension schematics

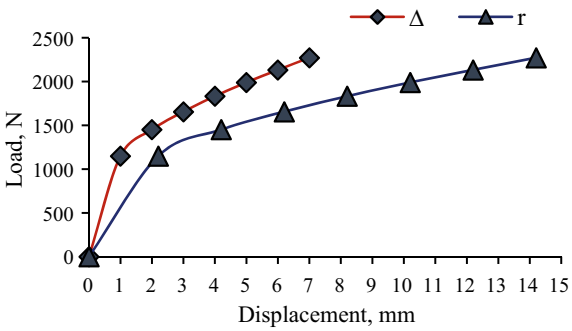

Fig. 3 The runner compression test results

The Skeleton runner was later tested in the laboratory to determine stiffness parameters. The experiment was performed using the material tension/compression equipment Zwick/Roell Z600. The Skeleton runner was fastened to the measuring device by fixing both of its ends. Deformations were measured after compressing the ends of the runner to compression distance Δ, registering the changing radius of curvature r, and the compression force F (Fig. 2). The resulting numerical values are shown in Fig. 3.

3 3D Frequency Analysis for Skeleton Sledge

Analyzing the effect of vibrations on the sliding motion on the ice surface it must first be clarified how the sliding object responds to the forced oscillations. To perform frequency analysis, it is necessary to simplify the model. In the Fig. 4 a simplified finite element skeleton sled model is showed. The screws used for runner fixing at the front are replaced by a pin connection in the model. The spring connection is used for runner stiffness modeling. The Direct Sparse solvers were used to consider the effect of loading on the natural frequencies and model have widely different material properties for skeleton sled parts. For FEM mesh type is Curvature based mesh selected with more than 4.9e4 elements.

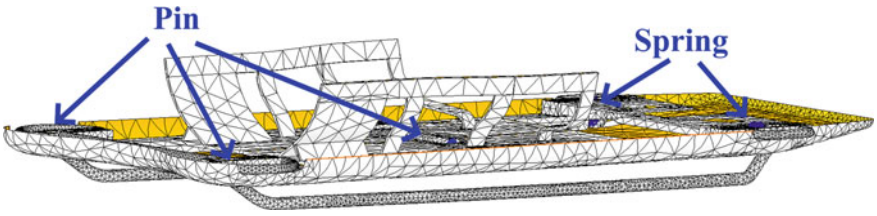

Fig. 4 Skeleton sled model with simplified connections

4 Mathematical Link Model of Resonant Frequencies for the Skeleton and Slider

For the determination of the natural frequencies of the Skeleton sleighs, a simplified one-dimensional model with 6 elements, which can be seen in Fig. 5, was created analytically. In this type of Link system elements are connected to each other by spring connections. The combined mass of sleigh and slider is M = 100 kg. It is divided symmetrically into two parts: M/2 = m1 = m6. The masses are flexibly connected with the spring of stiffness parameter c_2 describing the skeleton sleigh stiffness. The mass of the skeleton's runners is formed as m2 = m3 = m4 = m5 = 0.3 kg. The runners' elements are connected flexibly by the spring with stiffness parameter c_1.

In order to calculate the natural frequencies, the system of equations for all spring connections was compiled. In addition, some harmonic force was added to one element, in Fig. 5 example, the m3:

$$P_3 = P0 \cdot \sin(\omega \cdot t), \tag{1}$$

where *P0* –applied force, N;

ω –angular frequency of the oscillations, rad·s^{-1};

t – time, s.

Adding a harmonic force to the system initiates the forced oscillations. The magnitude of the force is not of critical importance in this case and therefore P0 was chosen to be P0 = 1 N. Since there is no damping in the system, all elements oscillate harmoniously with one angular frequency ω. Therefore, there is no need for the first derivation of the system to get the velocity. Obtaining the second derivation, the accelerations of the Link elements will be

$$\ddot{x}_i = -A_i \cdot \omega^2 \cdot \sin(\omega \cdot t), \tag{2}$$

where *A*—amplitude, mm;

i = 1, 2, 3, sequential number of mass elements.

From Newton's Second Law, for the Link system, after simplifications done the system of equations is obtained:

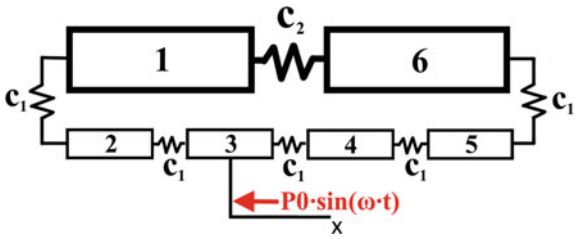

Fig. 5 The Skeleton and Slider Link Model

$$\begin{aligned}
&\frac{M}{2}\cdot\left(-A_1\cdot\omega^2\right)=-c_1\cdot(A_1-A_2)-c_2\cdot(A_1-A_6);\\
&m\cdot\left(-A_2\cdot\omega^2\right)=-c_1\cdot(A_2-A_1)-c_1\cdot(A_2-A_3);\\
&m\cdot\left(-A_3\cdot\omega^2\right)=-c_1\cdot(A_3-A_2)-c_1\cdot(A_3-A_4);\\
&m\cdot\left(-A_4\cdot\omega^2\right)=-c_1\cdot(A_4-A_3)-c_1\cdot(A_4-A_5)+P0;\\
&m\cdot\left(-A_5\cdot\omega^2\right)=-c_1\cdot(A_5-A_4)-c_1\cdot(A_5-A_6);\\
&\frac{M}{2}\cdot\left(-A_6\cdot\omega^2\right)=-c_1\cdot(A_6-A_5)-c_2\cdot(A_6-A_1).
\end{aligned}\tag{3}$$

By solving the equation system (3), it is possible to find accelerations for all elements of the amplitude outside the resonant frequencies. Accordingly, in the resonant zones, the amplitudes tend to infinity. This means that the determinant of the system (3) is equal to zero. From the equation of this determinant, by inserting $c_1 = F{\cdot}r^{-1}$ and $c_2 = F{\cdot}\Delta^{-1}$ (Fig. 3) one find:

$$\begin{aligned}
&-4.100625e71\cdot\omega^{12}+1.7027063782696177062e78\cdot\omega^{10}\\
&-2.3305500067588630372e84\cdot\omega^{8}+1.173048438913584662e90\cdot\omega^{6}\\
&-1.655977938480901193e95\cdot\omega^{4}+2.2677913365951951128e99\cdot\omega^{2}=0,
\end{aligned}\tag{4}$$

where ω—Eq. (4) roots, that correspond to the resonant frequencies.

5 Results and Discussion

Accelerometer recording signal from experiments on the ice track was processed using the Fast Fourier Transform (FFT) software. The resulting spectral graphs are shown in the following Figs. 6, 7, and 8. In experimental studies, the resonance frequencies characterizing the skeleton's and athlete's motion were recorded by an accelerometer. They correspond to the first peaks in the graphs of the acceleration components Ax, Ay, and Az and those are around 5–8 Hz.

The main factors influencing the occurrence of these resonant frequencies are the variable stiffness of the runner associated with environmental conditions, such as ice and air temperature, changes in air pressure, and humidity. The resonant frequency values vary nonlinearly and their shape is wavy if depending only on the stiffness. Only oscillations affecting the construction's structure were analyzed in this study. For example, Fig. 6 shows that the acceleration component Ax has no resonant peaks in the data signal. Accordingly, in the next Fig. 7, the transverse acceleration component Ay has a significant peak shape at 15 Hz. It is important to note here that the experiment was carried out on the ice track with a specially grooved control groove at a depth of about 2 cm (Fig. 2). This is necessary to ensure that the sleighs moved in a straight line. Thus, there is an explanation why the acceleration component Ay in

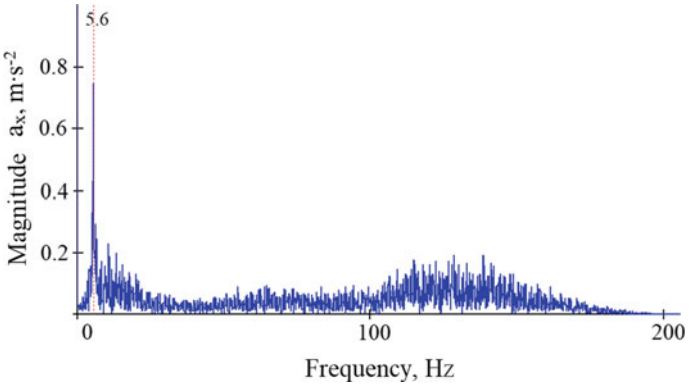

Fig. 6 Acceleration spectrum in x-axis direction

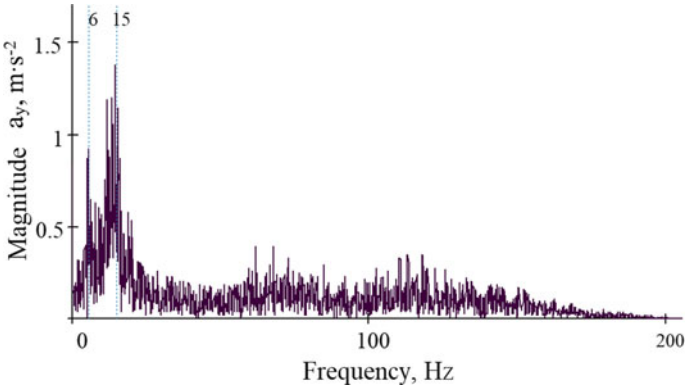

Fig. 7 Acceleration spectrum in y-axis direction

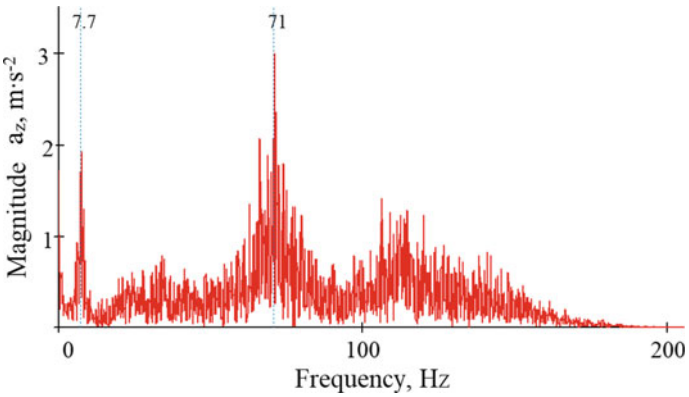

Fig. 8 Acceleration spectrum in z-axis direction

the y-axis direction has relatively high acceleration values, i.e., oscillations affecting both motion and construction forms appear.

From the analysis of experimental data records, the highest and most significant acceleration values are formed from the contact with the base. This is observed in the spectrum of the vertical component Az shown in Fig. 8. It has been experimentally determined how the runner's stiffness's parameter r influences the dispersion of the natural frequency measurements (Fig. 9). From the result obtained it can be concluded that the oscillations are on average with a frequency of about 71 Hz. The distribution of the mean value of the natural frequency is smaller and falls within the confidence interval.

In this study, the experimentally obtained resonant frequencies 15 and 71 Hz acceleration Ay, Az components were compared to the 3D model simulations. The results obtained are summarized in Fig. 10. The simulation has been done for five different cases. That is, the runner's tension r and the runner's stiffness Δ were varied from Low r = 6 mm and Δ = 3 mm to High r = 13 mm and Δ = 7 mm. The diameter of the runner cross-section, dr = 16 mm, was also taken into account when determining the stiffness of the runner. Results showed that changes in runner

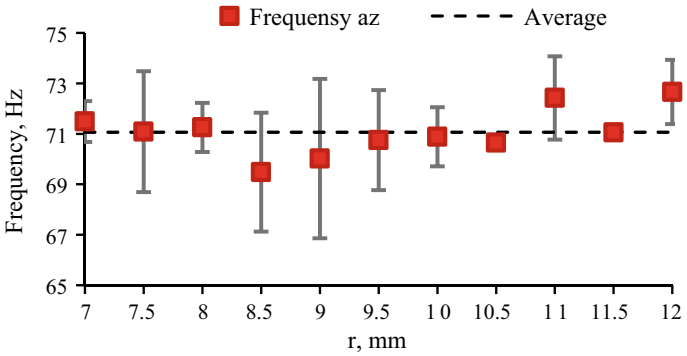

Fig. 9 Measured frequencies for skeleton sled structure vibrations in the z-axis direction depending runner stiffness radius r

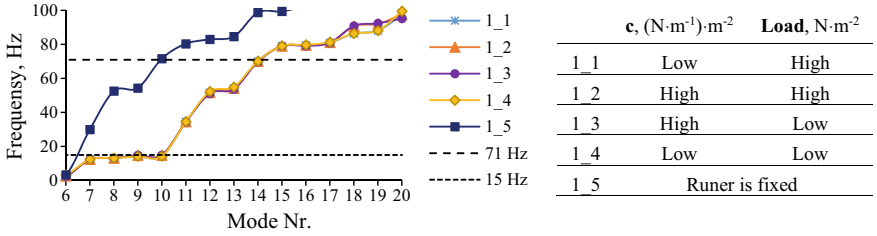

	c, $(N \cdot m^{-1}) \cdot m^{-2}$	**Load**, $N \cdot m^{-2}$
1_1	Low	High
1_2	High	High
1_3	High	Low
1_4	Low	Low
1_5	Runer is fixed	

Fig. 10 Results from 3D skeleton sled frequency analysis with different spring stiffness and rigid connection (fixed runner)

stiffness have a negligible effect on the natural frequency of the whole skeleton sleigh structure.

The results of 3D modeling show that increasing the spring tension increases the natural frequency. First twenty natural frequencies of the model were determined (Fig. 10). Similarly, 3D modeling results confirm that there is a good correlation between the natural frequencies' 15 and 71 Hz locations in the entire range of the 20 modes (Fig. 10).

The following additional conclusions and discussion points can be made from 3D modeling results:

1. A different result is obtained if the runner's spring's connection to the skeleton sleigh is replaced by a latching joint (curve 1_5). Here, the stiffness of the construction's structure increases and the number of low natural frequencies decreases. This is due to the elasticity of the skeleton's runner. The elastic behavior can be verified by observing the modes' shapes, while knowing that the first natural frequency of the runner is at 120 Hz (determined previously after detaching the runner from the system using a certified measuring device from the Microlog Gx series).
2. Modes from 7 to 10 at 15 Hz (see Fig. 10) and refer to the runner's oscillations in the axial direction as well as one rotational oscillation in the longitudinal direction. This proves that in the physical experiment, because of the ice grooves, the skeleton's runners produce such transverse oscillations that show the first natural frequency of the model.
3. The created program calculates different forms of oscillation, but only those that correspond to measurements from physical experiment are examined in detail.
4. The second natural frequency is the most significant, most pronounced frequency of self-oscillations, which is determined in the physical experiment at 71 Hz, and coincides with the calculated 3D model. This is also confirmed by the form of oscillations shown in Fig. 11.

This picture shows two cases in which the skeleton runner on the left is connected to a tensioned spring, while the runner on the right side is fixed to the frame. Accordingly, in the fixed case, the frequency increases by 1.5 Hz. Here, for the sake of visibility, the displacements are magnified.

The results of the analytical solution from the mathematical chain method model (Fig. 5) were obtained by solving Eq. (4) with the angular velocity ω argument function intersections with zero (Fig. 12).

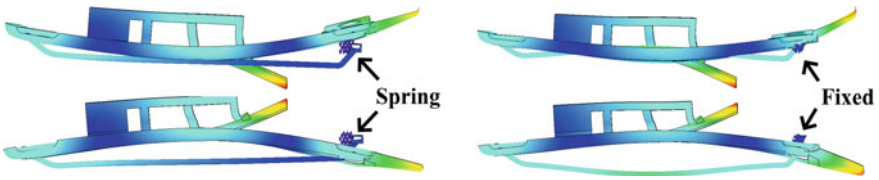

Fig. 11 Skeleton sled Mode shapes depending on connection type

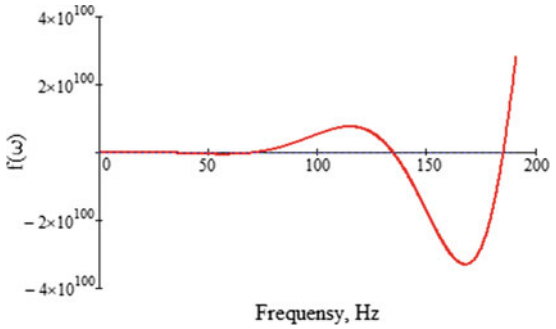

Nr	Frequency, Hz
1	0
2	19.69
3	71.13
4	134.63
5	185.13
6	217.57

Fig. 12 Angular velocity function cross points with zero and resonance frequencies

All six natural frequencies of the model were analytically determined. The first is equal to zero because there is no external elastic force. The second is 19.6 Hz, which is 4 Hz higher than that found in the physical experiment and 3D simulations. In turn, the main third natural frequency, which is 71.13 Hz, coincides with both physical experimentation and 3D simulation calculations. To explain the discrepancy should be noted that the mathematical model is 1D and does not consider transverse oscillations.

6 Conclusions

1. From the results of the experiment, it can be concluded that when changing the tension of the runner, the skeleton sleigh's structure's natural frequencies 15 Hz and 71 do not change in the time of the motion.
2. The results of 3D modeling show that changing the stiffness of the runner reduces the number of free oscillations.
3. The developed 6DOF mathematical model for determination of natural frequencies of the skeleton sleigh construction allows easy and quick determination of approximate natural frequencies knowing the skeleton runner's stiffness' values.
4. The accuracy of the proposed mathematical model can be improved by increasing the number of DOFs and additionally adding damping.
5. An algorithm has been developed which allows setting the optimum runner's tension of the skeleton sleigh before start, depending on the athlete's weight.

Acknowledgements This work has been supported by the ERDF project "The quest for disclosing how surface characteristics affect slideability" (No.1.1.1.1/16/A/129)

The authors gratefully acknowledge the assistance from Dainis Dukurs, Inga Reiniņa, Ernests Jansons, and Liene Pluduma for assistance with experiments at the bobsled push-start facility.

References

1. International Bobsled and Skeleton Federation: International Skeleton Rules 2018 https://www.ibsf.org/en/downloads
2. Irbe M, Gross KA, Viba J, Cerpinska M (2018) Analysis of acceleration and numerical modeling of skeleton sled motion. Eng Rural Dev 17:1401–1406. https://doi.org/10.22616/ERDev2018.17.N179
3. Braghin F, Cheli F, Melzi S, Sabbioni E, Maldifassi S (2016) The engineering approach to winter sports. The engineering approach to winter sports. Springer New York, pp 1–383. https://doi.org/10.1007/978-1-4939-3020-3
4. Lehtovaara A (1987) Influence of vibration on the kinetic friction between plastics and ice. Wear 115(1–2): 131–138. https://doi.org/10.1016/0043-1648(87)90204-3
5. Shionoya A, Shimizu Y, Kenmotsu Y, Imamura A, Uchiyama H, Kimoto R, Kawada K (2015) Development of new simulator generating high frequency component of ski board vibrations in actual skiing. Procedia Eng 112:379–384. https://doi.org/10.1016/j.proeng.2015.07.211
6. Hess DP, Soom A (1991) Normal vibrations and friction under harmonic loads: part i—hertzian contacts. J Tribol 113(1):80–86. https://doi.org/10.1115/1.2920607
7. Hess DP, Soom A, Kim CH (1992) Normal vibrations and friction at a Hertzian contact under random excitation: Theory and experiments. J Sound Vib 153(3):491–508. https://doi.org/10.1016/0022-460X(92)90378-B
8. Roberts I (2013) Skeleton bobsleigh mechanics: athlete-sled interaction. Ph.D. thesis. The University of Edinburgh. https://www.era.lib.ed.ac.uk/handle/1842/7600
9. Dassault systemes solidworks corporation: solidworks simulation premium: dynamics (2018), pp 1–178
10. Akin JE (2010) Finite element analysis concepts: via solidworks. Finite element analysis concepts: via solidworks, pp 1–335. https://doi.org/10.1142/7785
11. Kurowski PM (2016) Vibration analysis with solidworks simulation. SDC Publications Mission, KS
12. Lalanne C (2010) Mechanical vibration and shock analysis: second edition. Mechanical vibration and shock analysis: second edition, vol 4, pp 1–436. https://doi.org/10.1002/9780470611968
13. Newland DE (1993) An introduction to random vibrations, spectral and wavelet analysis, 3rd edn, pp 1–477. https://doi.org/10.1155/1994/561605